UNSYS digital

International Journal of Robotics and Mechatronics

Piezoelectric Ultrasonic Servo Control Feed Drive Renovate Electro-Discharge Machining System Industrial Applications and Transfer the Technology into a New Era

Mahmoud Shafik

School of Engineering and Technology, University of Derby, Derby, United Kingdom

***Abstract*—**This paper presents the state of art of the latest development in Electro-Discharge Machining (EDM) system technology. It covers the current and recent development using the electromagentic and piezoelectric ultrasonic servo control feed drive technology. The paper also demonstrates how the ultrasonic technology renovates the system and transfers its industrial applications into a new era. EDM process is one of the most common processes in automotive and aerospace industry. It is mainly used to machine and process alloys and very hard materials for key manufacturing components, such as film cooling holes for Turbine Blades, engine strip sheets, steel sheets for automotive industry, outer vehicle body, … etc. The EDM system that uses electromagnetic servo control feed drive has a number of teething issues and this indicated the necessity to employ a new technology that could overcome these issues and enhance the system level of precision, dynamic time response, machining stability, arcing phenomena and product surface profile. The research undertaken to evaluate both systems showed that the system recently developed using ultrasonic servo control feed drive has a clear improvement in system dynamic time response, stability, a notable reduction in arcing and short-circuiting teething phenomena. This has been verified through the inter-electrode gap voltage variation. The electron microscopic examinations into the machined samples using the ultrasonic system have also indicated a clear improvement in the surface profile of the machined samples.

***Keywords*—**Electro-Discharge Machining, Industrial Automation, Mechatronics, Servo Feed Drive, Electro-Mechanical System.

I. Introduction

Electro Discharge Machining (EDM) system have been known since 1940's. It has been used in many industrial application, especially in aerospace and automotive industry. EDM applications are classified as high precision machining and surface treatment process. It is very well known that higher accuracy, fine resolution and fast dynamic response are essential parameters for high precision machining and manufacturing processes. The main principle of operation of EDM is based mainly on a spark discharge between two conducting surfaces separated by a dielectric medium. The generated spark duration is on the order of microseconds and the inter-electrode gap size is of the order of 10 to 100 micrometers [1]-[8]. EDM is widely used in various applications including machining different complex and intricate shapes, slots, drilling holes, cutting and texturing [1]-[11]. The actual texturing process well-known as Electro-Discharge Texturing (EDT) generally has a multi-rotary motor/ballscrew/slide/slideway arrangement in a small volume [4], [12]. The function is to focus as many electrodes on a given area as possible, given the limitations of the design constraints that is dominated by the physical size and volume of electric servomotors and the other kinematic elements required to effect rotary to linear motion. Texturing is a process of creating irregularities, with regular or irregular spacing that tends to form patterns or texture on the surface. Texture contains roughness and waviness that can assist in providing inherent quality of any subsequent paint finish, appearance and lifetime. Since the requirements of high precision and accurate machining process of EDM and EDT applications never stop rising, much of the research has been concerned with the servo control feed drive level of precision, stability, dynamic time response and surface profile of the processed products and surfaces. Some authors have identified these problems and a number of investigations into the electric servomotor system have been carried out [13]-[15]. However, success in presenting a realistic solution to these issues has been limited. Consequently, there was a need to develop a new servo control feed drive using innovative emerging technology that could provide high precision, fast dynamic response, robust stability and meet the process design specifications.

Piezoelectric ultrasonic (USM) servo feed drive technology offers many opportunities in the field of high precision servo positioning control, fast dynamic time response and robust stability [15]-[17]. These criteria give them the potential to replace electric servo motors arrangements in a number of

Corresponding author: Mahmoud Shafik (e-mail: m.shafik@derby.ac.uk).
This paper was submitted on December 30, 2013; revised on June 09, 2014; and accepted on June 09, 2014.

industrial applications [9], [11]-[12], [18]-[20]. It has also been used widely in both instrumentation and smart machine tool industrial applications such as, EDM [20], EDT [4], [12], micro-machining [1]-[3], classification for a prosthetic forearm [21]-[22], auto focusing drives for single-lens reflex cameras [23], rotary supports for video cameras and artificial heart actuators. These applications shows that piezoelectric USM servo control feed drive systems technology can be more effective than electric servomotor drives whenever high and ultrahigh precision level of control is required. This is due to their high resolution, high stiffness, large output force, compactness and quick dynamic time response despite their limited positioning ranges. The piezoelectric ultrasonic servo drive structure principally depends on the industrial application design specifications [11]-[12], [21]-[33]. Potentially, they offer a significant flexibility for position and feed-rate control [34]-[37]. They have compact size, high force density, simple mechanical construction, low weight, slow speed without additional gear or spindle, high torque, non-magnetic operation, freedom for constructional design, very low inertia, fast dynamic responses, direct drive, fine position resolution, miniaturization and noiseless operation [38]-[39].

Demanding and careful examination for these applications reveals that there are apparent shortcomings. The first shortcoming is in regard to the dynamic time response of the motor and its transfer function. While a piezo-ceramic element (typically Lead zirconate titanate (PZT)) expands in direct proportion to the magnitude of the applied voltage, the USM on the other hand accumulates those displacements over time. Therefore the transfer function of the USM, related to the magnitude of the driving signal to the displacement is an integrator [40] and this shows a delay in the dynamic response of the USM, but it is not nearly significant as that in an electric servomotor. The second shortcoming is that because motion is transmitted through a friction force between solid elements, it will have a dead band due to the friction. Often USM does not move until the electrical input signal is greater than 10% of the maximum allowed voltage to overcome the friction. Such a dead band limits the ability of a USM to accelerate quickly and position accurately [9], [12], [18]-[20], [40]. These USM unique features and even these shortcoming still presents a real opportunity to implement USM servo control feed drive technology to improve EDM servo control system degree of precision, dynamic response, performance and extend its capabilities to include more accurate machining. This is in addition to its direct drive, fine position, high resolution, compact size in comparison to the electric servomotors, same kinematics capability as a rotary motor-ballscrew-slide-slideway arrangement, and is controllable within the limits that electric servos motors operate [41]-[42].

In this paper, the first section provides an overview of the electric servo control feed drive technology in use for EDM and issues associated with it. It also demonstrates the potential advantages that piezoelectric ultrasonic servo control feed drive technology can offer. The second section provides the recently developed system using piezoelectric ultrasonic servo control feed technology. The third section provides an evaluation of both systems using electric and ultrasonic technology. Section four provides an analysis and discussion. The paper ended with a conclusion showing how the new system using ultrasonic servomotor technology has overcome the electric servomotor EDM drive system teething issues and transfer the technology into a new era.

II. USM Servo Control Feed Drive

The overall design of the USM servo drive has considered the EDM and its various industrial applications application design specifications and needs. This includes type of motion, degree of resolution, travelling speed, output force, load capacity, torque, compactness, and integration of the parts into the frame of the drive, production of the various parts, maintenance and sustainability. The design process of the USM servo feed drive system have passed through a number of phases. The first phase focused on the actuator design and structure that meets the EDM application requirements. Second phase focused on the finite element analysis and principles of motion, elements design, fabrications and the final phase focused evaluation of the potential parameters such as electric parameters, load capacity, feed/travelling speed rate and dynamic time response. The final phase focused on electronic driver and control unit design and development.

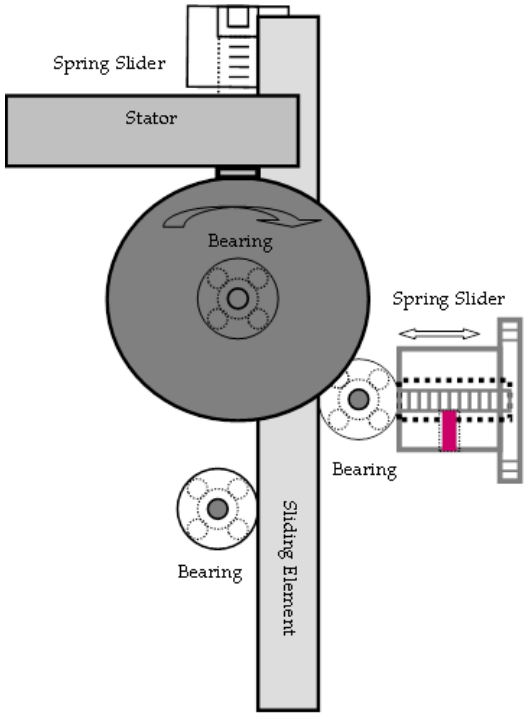

Figure 1 USM servo control feed drive actuation system using a single flexural vibration transducer for EDM industrial applications [9], [11]-[12], [18]-[20]

A. Structure of USM Drive Actuation System

The dual mode standing wave USM drive actuation system consists of three main parts: the stator, rotor, and sliding element. The stator is a single flexural transducer made from

PZT piezoceramics material. The rotor is composed of the servomotor drive driving wheel and the shaft. The sliding element is made up of rectangular tube steel. The stator, rotor and sliding element jointly with the frame of the USM actuation system form the linear structure of the USM servo drive. **Figure 1** shows the USM drive structure.

B. Working Principles of the USM Actuation System

The working mechanism of the USM servo drive actuation system is based on creating elliptical micro motions of surface points generated by superposition of longitudinal and bending vibration modes of oscillating structures [18]-[20], [29]-[30]. By pressing the rotor against the driving tip of the stator, the micro elliptical motions are converted into a rotary and then to linear motion, through the friction between parts of the servo drive actuation system. However, to create a strong second bending vibration mode, the polarisation direction of the PZT piezoelectric vibrator must be made perpendicular to the electrodes, the piezoelectric ceramic vibrator was arranged as shown in **Figure 2**. The longitudinal and bending vibration modes are coupled by asymmetry of the piezoelectric ceramic vibrator [28], [39]-[41].

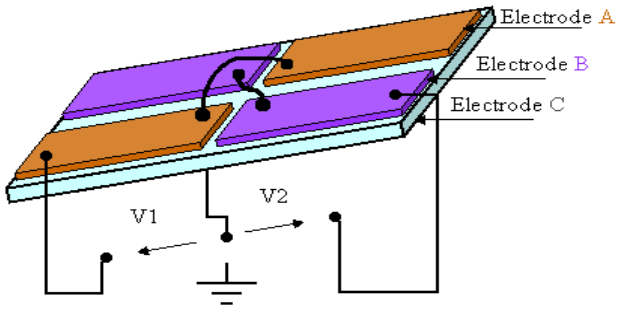

Figure 2 USM Actuation UNIT stator connections arrangements and principles used to generate bidirections of motion [18]-[20]

The first surface of the piezoelectric transducer is segmented into four sub-surfaces which are arranged electrically to provide two sub-electrodes, named A and B. The second surface is grounded and named electrode C. Then a single-phase AC signal with a wide frequency band is used to obtain the electrode natural operating frequency. Driving the electrode A and C by a single phase AC signal with a frequency closer to the natural frequency of the PZT transducer provides one direction of motion and switching to electrode B, and changes the bending vibration mode by a phase shift of 180 degrees, which leads to reversing the direction of motions. Few authors have used these phenomena and succeeded to develop different structures to generate linear and rotary motion [18], [28]-[29], [41]-[43]. Snitka V. (2000), and Aoyagi M. (1992), showed that the load of this type of actuator depended on the contact point of the rotor, the dimension of the piezoelectric elements and material of the stator and the rotor. Snitka V. (2000) proved that the pre-load pressing forces and friction between parts influenced the degree of position accuracy that can be obtained. Therefore, the material for the moving parts of the servo feed drive were carefully selected.

The servo drive USM actuation system was designed using standing wave vibrations with a fixed wavelength. The perception is to utilize two oscillation modes of vibration to obtain desired motion of the piezoelectric vibrating transducer longitudinal and transverse vibration modes. One vibration produces a normal force, while the other vibration generates thrust force that is perpendicular to the normal force. This leads to a micro elliptical trajectory of motion, at the vibration transducer tip, by attaching the stator tip to the rotor unit using an adjustable coil spring. The micro elliptical trajectory is converted into a rotary motion. As the combination of two modes of vibrations created a friction-based driving force between the stator and the rotor at the contact tip, a movement in forward or backward direction was created depending on the methodology used to electrify the piezoelectric ceramic transducer to generate two modes of vibrations. The linear motion was developed using the friction based driving force between the shaft and the sliding element of the USM servo drive unit as shown in **Figure 1**.

C. Modelling and Experimental Evaluation of the USM Actuation System

Piezoelectric USM's actuation technology has many complex non-linear characteristics, and modelling them is an essential step of the design and development lifecycle. There are two methods of modelling, and analysis can be used to simulate and model piezoelectric USM's [44]-[46]. These methods are the analytical analysis and finite element analysis (FEA) method. In the USM servo control feed drive development process, ANSYS FEA software was used to examine the actuator structure, investigate the material vibration modes, identify the transducer material, and obtain the technical operating parameters. It also helped to optimise the actuator performance through investigating the variation of the displacement versus the frequency. ANSYS software offers more than a hundred different types of finite elements. Each element can define a set of materials according to their physical characteristics. In this model SCALAR98 TET (tetrahedral couple field solid element) coupled field finite element was used to define the piezoceramic material. It has ten nodes with row degree of freedom per node and suitable for different loads. The solutions for this element are obtained in two ways, Nodal DOF which includes all nodal solutions and additional output element parameters. SOLID72 structure finite element with rotation (SOLID72-4-node tetrahedral structural solid with rotation) was used to define the passive element. It has four nodes and six degrees of freedom. CONTAC49 contact element is chosen to identify the contact element and to complete the realisation of the model. It has five nodes, with three degrees of freedom per node and has the capability to represent the general contact of models that are generated with arbitrary meshes. It also has the ability to represent and identify point to surface contact and sliding between the two contact surfaces in three dimensions. CONTAC49 contact element is sometimes applied for contact of solid bodies or shells, to static or dynamic analysis, to problems with or without friction and to flexible-to-flexible or rigid-to-flexible body contact. So, it allows elastic and inflexible friction. Two types of FEA were used, modal analysis and harmonic analysis. These offer two types of loads, the nodal and the pertaining to the element. In the nodal case, the loads were applied to nodes of the element that do not have direct links with element properties. The USM models were built based on a full consideration of the actuator

boundary conditions and EDM industrial application requirements. The stator was defined as the active element and the rotor was defined as the passive element. **Figure 3 (a)**, **(b)**, **(c)**, and **(d)** show the variation of displacement of the stator on x, y and z direction versus the frequency, for actuator linear structure. It illustrates the change of displacement versus the frequency, and also shows the resonant frequency of the current model equal to 42.2 kHz. This helps to determine the displacement amplitude, thrust force and optimal actuator structure performance.

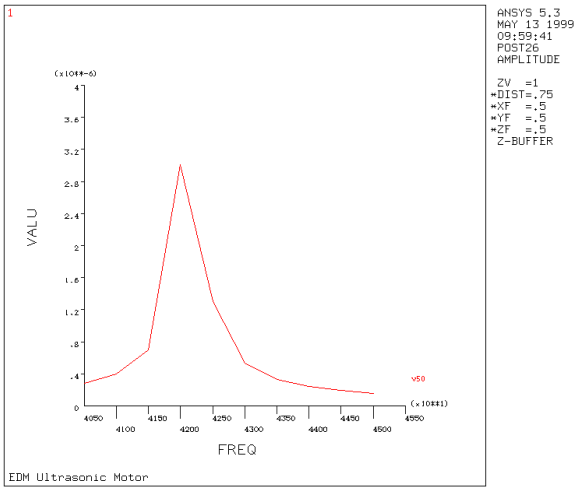

(a) The resonance displacement variation vs. exciting frequency

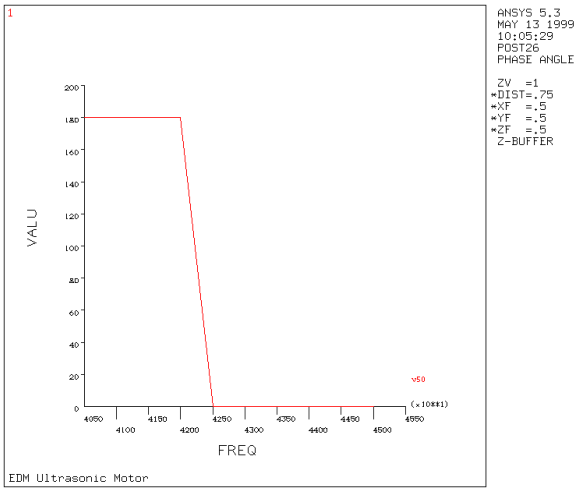

(b) The phase variation vs. frequency

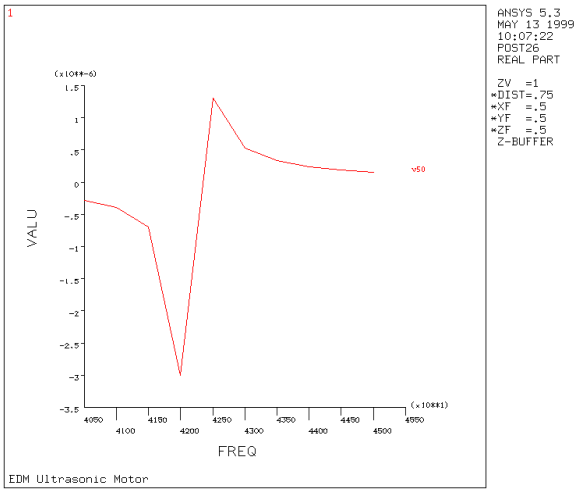

(c) The real part of the resonance displacement variation vs. frequency

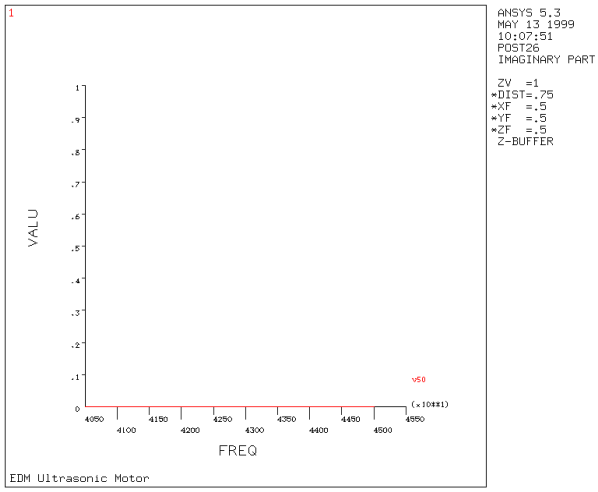

(d) The imaginary part of the resonance displacement variation against exciting frequency

Figure 3 The USM servo control feed actuation system (50 volt)

The resonance displacement amplitude here was obtained using the following relationship:

$$RD_p = \alpha dEL \tag{1}$$

where: RD_p is the resonance displacement; α is the amplification factor, and this is a function of quality factor Q; d is the piezoelectric constant; E is the applied electric field; and L is the length of the PZT sample.

The USM servo feed drive arrangement modal analysis result has shown some influences of the sliding element on the transducer deformation modes of vibration and the possible maximum resonance displacement. The displacement of the transducer changed from 10.1125 µm for the rotary structure model to 3.0999 µm for linear structure. The analysis enabled the assessment on the actuator possible generated amplitude of vibration, thrust force, material modes of vibration and the distribution of the vibration wave of the transducer, which helped to avoid design errors and mishandling of the material deformation. Material deformation can produce a jerking effect that affects the resolution, degree of accuracy, and the servo drive fine position, as a whole. The linear model structure has been investigated by applying a signal with various amplitudes at the obtained operating frequency. **Figure 4 (a, b,** and **c)** and **Figure 5 (a, b,** and **c)** show the two modes of vibration, in x, y and z, for the linear structure of the actuator: the transverse bending mode and longitudinal mode, at the natural operating frequency.

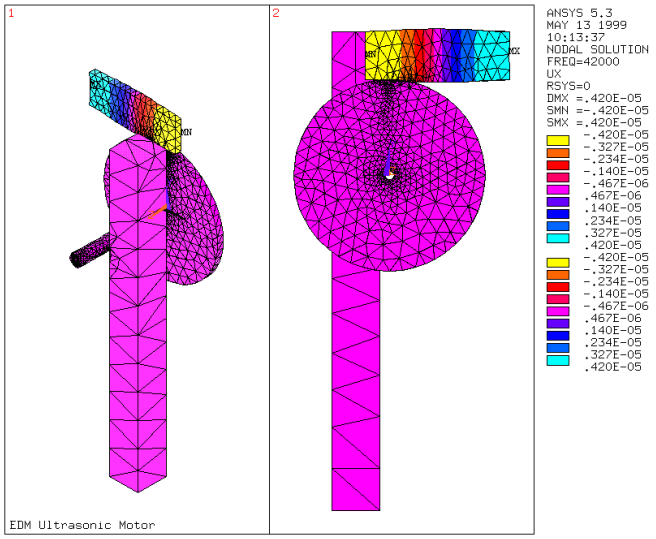

(a) X-direction (50 volt)

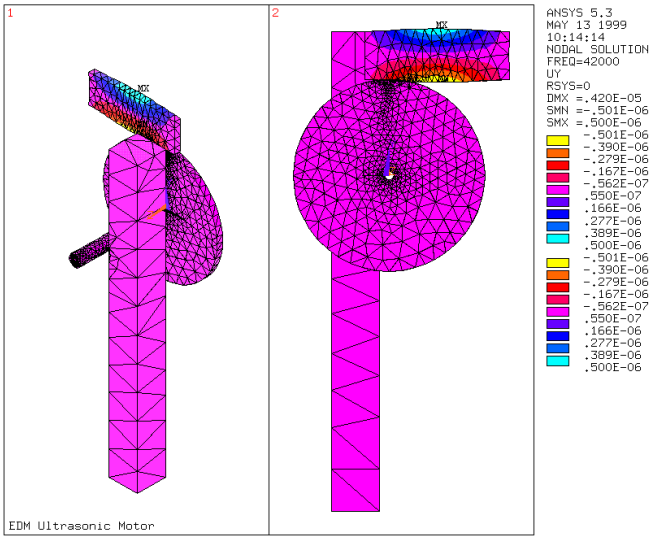

(b) Y-direction (50 volt)

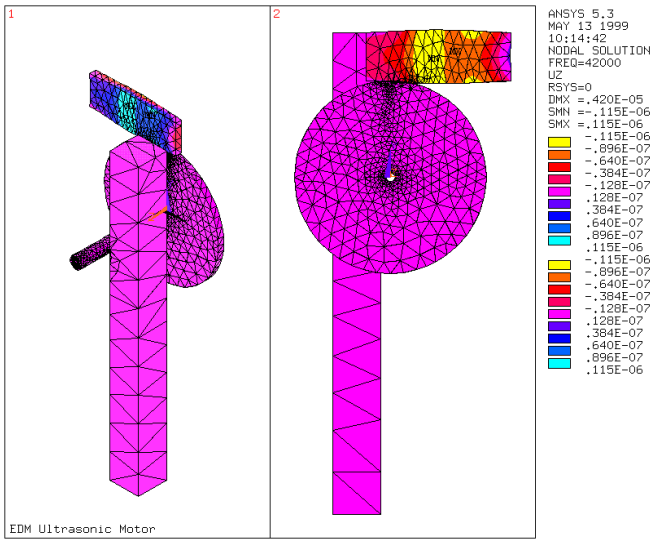

(c) Z-direction (50 volt)

Figure 4 Deformed shape for the real part of the input for the USM actuator System at the operating frequency 'mode (1)

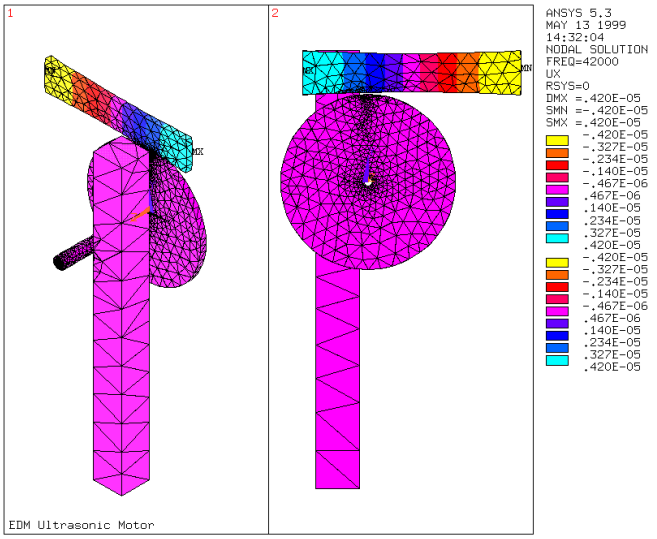

(a) X-direction (50 volt)

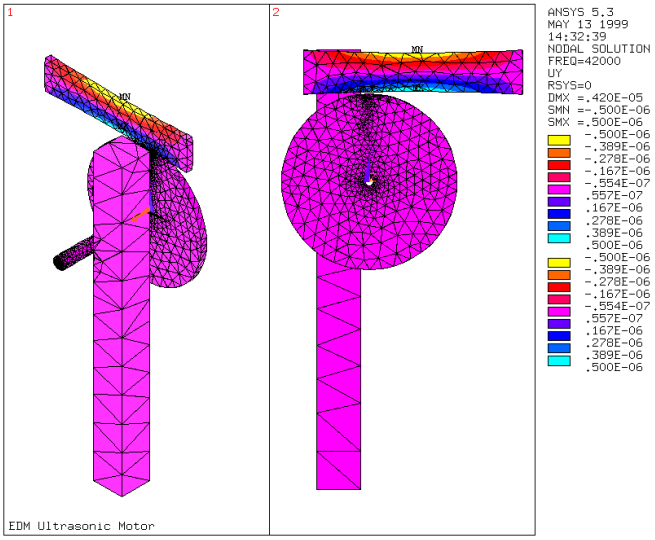

(b) Y-direction (50 volt)

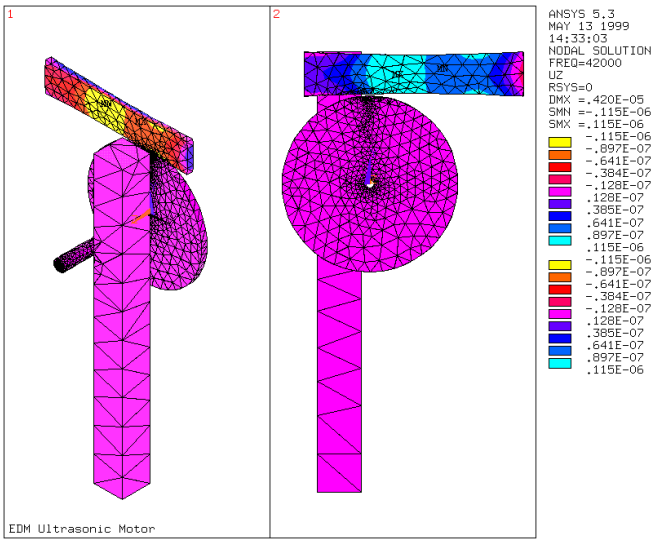

(c) Z-direction (50 volt)

Figure 5 Deformed shape of the real part of the input for the USM actuator system at the operating frequency 'mode (2)

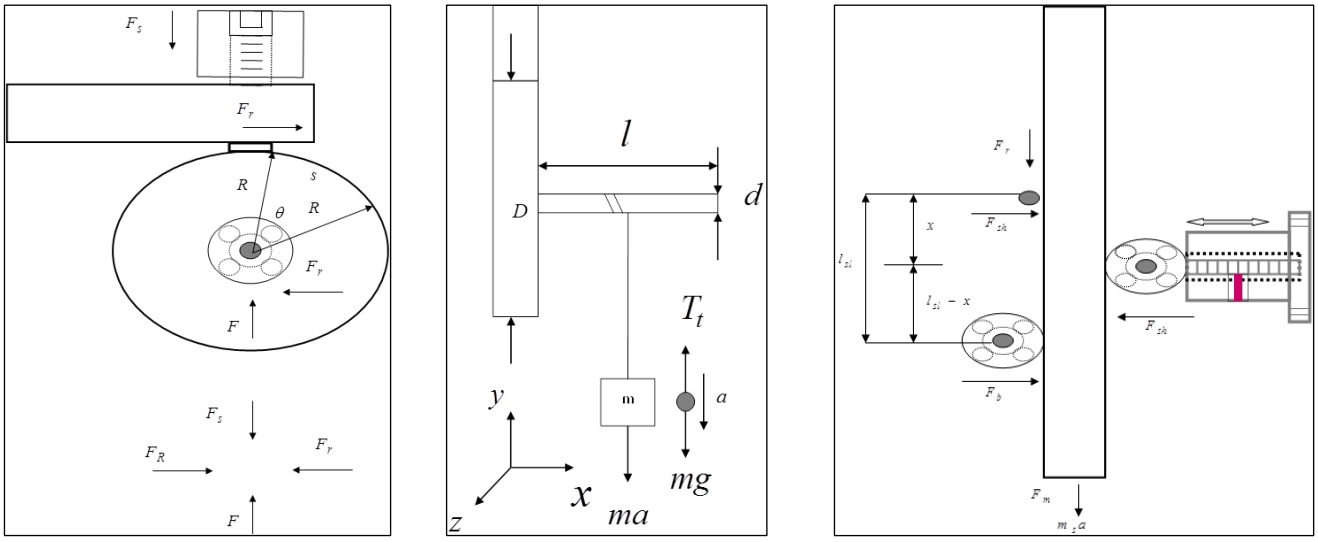

(a) **(b)** **(c)**

Figure 6 USM drive dynamic models used to determine the dimensions of the USM parts and to optimise the bearing preload force on the USM actuation system linear structure [9], [11], [18]-[20]

The dimensions of stator for the proposed USM were based on the ratio between the frequency of the longitudinal mode f_L and the frequency of the bending mode f_B, $\frac{f_L}{f_B} = 2.0$, and $\frac{d}{l} = 0.1$, as the internal nonlinear coupling of parametric vibration between two resonance modes was generated under these conditions [9], [11], [18]-[20].

The capacitance ratio and direction of vibratory displacement was also considered. Using the USM models shown in **Figure 6 (a)** and **Figure 6 (b)**, the relation between the torque T and various acting forces on the rotor components gives the following relationship:

$$T = F_R \frac{D}{2} = F_r \frac{d}{2} \tag{2}$$

where F_R is the micro-elliptical force produced using vibration transducer; F_r is the driving force transferred to the shaft using the following torque factor relationship $A_r = \frac{D}{d}$, where D is the diameter of the driving wheel, and d is the diameter of the shaft.

The torque factor of the USM and the diameter of the rotor (driving wheel and the shaft) were obtained. The transferred force to the shaft was determined using the following torque factor relationship:

$$F_r = F_R \frac{D}{d} \tag{3}$$

This relationship shows that the torque factor A_r has to be carefully considered during the design process of the USM since it influences the efficiency of the driving force produced by the vibration transducer, the resolution of the actuator, and maximum travelling speed.

The length of the shaft l_S was determined according to the allowable ratio of the $\frac{l_s}{d_s}$, where d_S is the diameter of the shaft. This is to meet the conceptual view of the design for the actuator construction considering the properties of the material used to produce the shaft and considering the moment of inertia of the rotor that was considered to be small for fast dynamic time response, and to obtain a maximum efficiency of the transferred driving force.

The pre-load force acting on the shaft and locations of bearings of the sliding element was determined using the dynamic model shown in **Figure 6 (c)**.

$$\sum F_x = 0.0$$

$$F_{sb} = F_{sh} + F_b \tag{4}$$

where F_{sb}, F_b, F_{sh} are the side spring slider, bearing and shaft acting forces, respectively.

From the model shown in **Figure 6 (c)**, the bearing acting force F_b was obtained from the following relationship:

$$F_{sb} X = F_b l_{sl} \tag{5}$$

Consequently, the bearing acting force was found to be:

$$F_b = F_{sb} \frac{X}{l_{sl}} \tag{6}$$

Substituting F_b into slider acting force:

$$F_{sb} = F_{sb} \frac{X}{l_{sl}} + F_{sh} \tag{7}$$

Then the shaft acting force was determined using (8):

$$F_{sh} = F_{sb} \left(1 - \frac{X}{l_{sl}} \right) \tag{8}$$

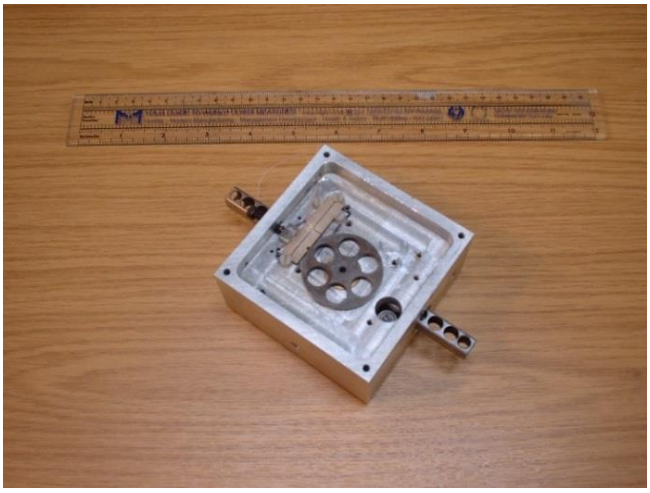

Figure 7 USM servo feed drive actual actuation system using a single piezo-ceramic flexural vibration transducer

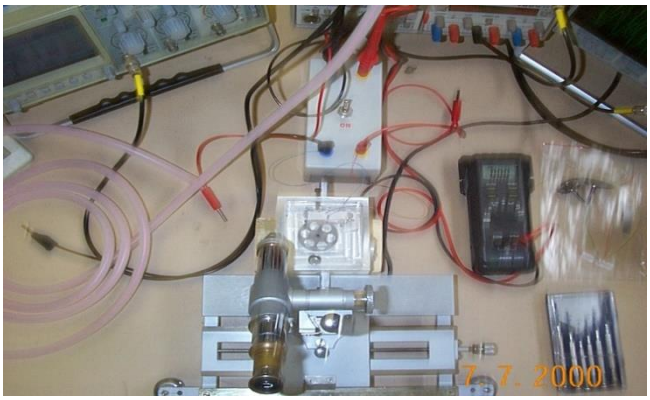

Figure 8 Actual test rig arrangement used to test and measure the characteristics of the developed USM Servo Feed Drive

In the design, the right-hand side spring of the bearing was located in the middle between the shaft and opposite left-hand side bearing, to keep the acting force on the shaft as minimum as possible. The optimised acting force on the shaft in this case was equal to half the slider pre-load acting force. Four pins and an exchangeable coil spring were used to house the vibration transducer. The four pins were used to prevent interference to transducer modes of vibrations. The coil spring was used to support the vibration transducer at the vibration tip as well to keep the stator and rotor in contact. This enabled the vibration transducer to transfer the micro-elliptical force into rotational and linear motion using the friction between the USM parts. The optimum pre-load acting force was determined by observing the USM travelling speed versus various forces at the identified operating parameters i.e. voltage, current, and frequency. It was noticed that mishandling of the preload acting force influenced the actuator resolution, stiffness and torque. Two guide-ways were also designed and fixed to the top and bottom of the USM frame in order to prevent the sliding element plane motion. Plane motion would affect the accuracy of the USM. The frame of the actuator is part of the concept, and was designed with a reliable layout to ensure compactness of the design, easyness to integrate, and to maintain the parts of the USM. **Figure 7** illustrates the USM manufactured prototype, and **Figure 8** shows the arrangement used to evaluate the USM drive actuation system. It was also observed that the slide element did not move until the operating voltage reaches about half of the maximum value. This reduced the fine micro resolution of the USM and affects its dynamic time response. The thrust force must overcome the static friction force between the actuator parts to allow relative motion between the stator and the rotor [35]. In this design a coil spring has been used to enable the pre-load force to be sensitively adjusted and minimize such issue.

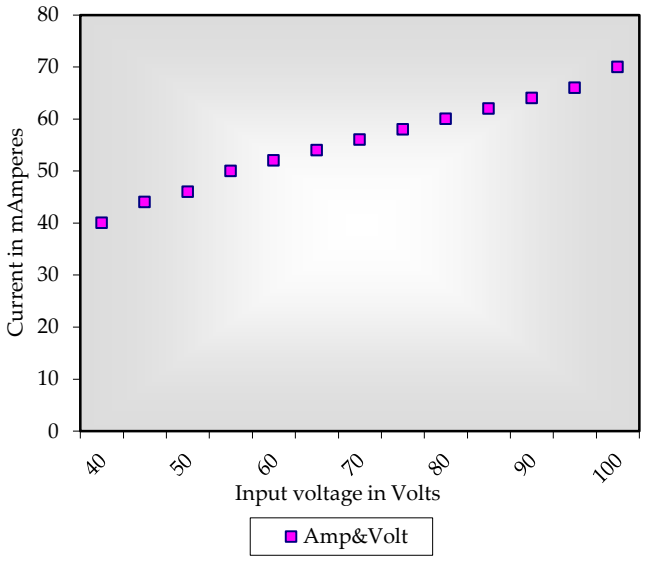

Figure 9 The variation of the current vs. input voltage for the developed USM Servo Feed Drive (no-load applied) [9], [11]-[12]

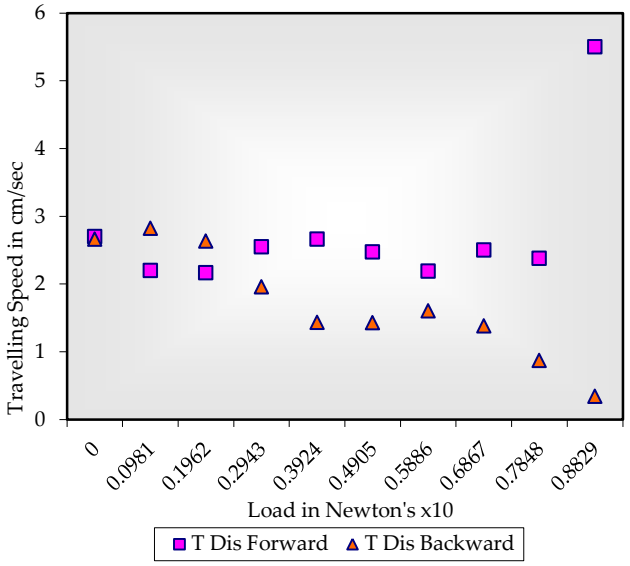

Figure 10 The variation of the travelling speed vs. applied load for the developed USM Servo Feed Drive [9], [11], [18]-[20]

Figure 9 shows the relationship between current and voltage of the prototype. This helps to identify the nature of the USM impedance and obtain the USM operating voltage and current.

The experimental test show that the prototype electrical operating parameters was found voltage equal to 50 to 100 volts and current equal to 50 to 100 mA.

The travelling speed versus the amplitude and frequency of the AC input signal was measured. This was achieved by arranging the system as shown in **Figure 8**. The frequency of USM driver was altered incrementally. Then the speed of the USM was measured for each increment. It was noticed during this process that the speed of the USM increased as the frequency of the driver increased, and at one stage, the USM reached a maximum speed, and then started to decrease dramatically. The variation of the travelling speed versus the applied load was also measured at various loads, and this is shown in **Figure 10**. This shows that the USM servo is drive able to carry a load up to 1.8 Newton which meets the requirements for industrial applications. It also shows that the USM drive was able to provide a feed/travelling rate/speed of 28 mm/s, and a resolution on the order of micrometers. The drive has two motion directions with un-similar characteristics as shown in **Figure 10**, as well as a wide range of frequency which enabled the control over the speed of the actuation system. The varying frequency or the amplitude of the input signal controlled the traveling speed of the USM [9], [11], [18]-[20].

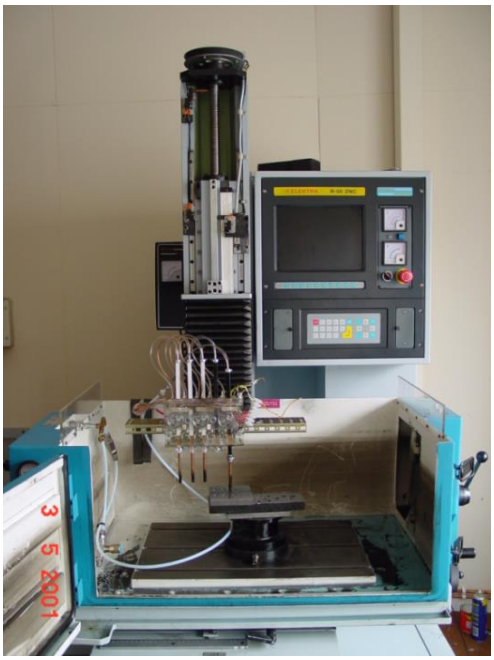

Figure 11 The USM servo feed drive installed in the EDM machine (A ELEKTRA R-50 ZNC MODEL)

III. EDM Systems Evaluation

The EDM systems using electric and USM servo control feed drive was evaluated. This evaluation process included an investigation into the stability of the system, capability of control, processing time and surface finish of the machined products. Various electro-machining parameters, including level of current, on/off time and duty cycle were used in this investigation. **Figure 11** shows both systems integrated into EDM A ELEKTRA R-50 ZNC model.

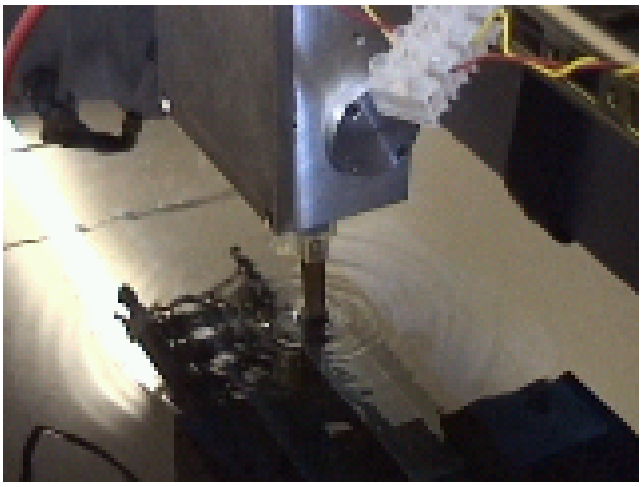

Figure 11 EDM Machining process using USM servo control feed drive system

Figure 12 Different holes machined using developed system of control and existing system using various electrical machining parameters

The current system using DC servo feed drive was used for machining different areas using various electro-machining parameters. Then the USM drive system was used for machining similar different areas by means of the same electro-machining parameters and conditions as shown in **Figure 13**. The levels of current, on-off time and duty cycle were used as main electro-machining parameters. The other machining parameters were selected as follows: The feed rate of the system in the case of auto position was 0.656 mm/sec, speed of the roll was 6 rpm, SEN = 1:3 [Sensitivity of Z-axis speed], ASEN = 3-9 [Antiarc sensitivity], TW =1.0 μsec [Sparking time], T = 0.5 μsec [Lifetime], Vg = 38: 50 volts [Gap voltage], Ig = 5 amperes [Gap current], Ib = 0.0 [Prepulse spark current], POL = -ve [Polarity of machining] and Fp = 0.2 bar [Flushing pressure]. The feed rate in the case of the piezoelectric ultrasonic control system was of the order of 5.1 mm/sec.

IV. Results and Discussions

The ultrasonic and electromagnetic control systems were evaluated. This evaluation included dynamic time response, machining stability, arcing phenomena and product surface profile. The stability of the EDM system can be distinguished from the inter-electrode gap voltage and current. This is in addition to the control signal obtained from the system control unit. Therefore, the feedback signal and inter-electrode gap voltage variation were obtained at various electro-machining parameters. **Figure 14** and **Figure 15** illustrate the variations of these signals for various electro-machining parameters for both control systems. It showed the indication of the stability of machining for a period of 10 seconds. **Figure 14** shows these variations for the existing control system using electric actuator. Here, it is notable that there is a clear instability on the feedback signal and the inter-electrode gap. **Figure 15** shows the variation in the feedback control signal and inter-electrode gap voltage for the USM servo feed drive system. This shows the stability of machining, remarkable reduction in the arcing and short-circuiting processes, which in turn leads to a clear reduction in the machining time when compared to the current system.

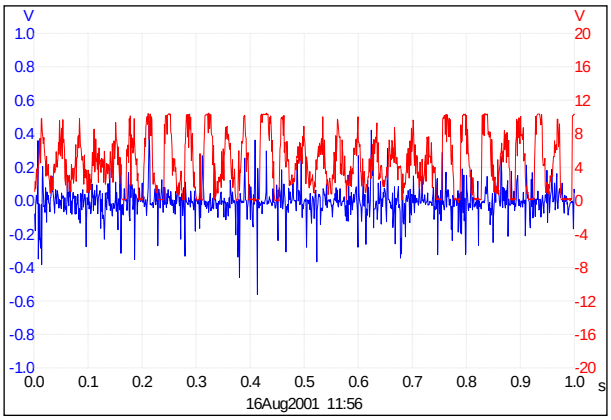

Figure 13 Feedback control signal (red) and inter-electrode gap voltage (blue) variation for EDM machining using the current dc servo control system (gap current 5 A, gap voltage of 38 volts & duty cycle 4 μsec) [10]

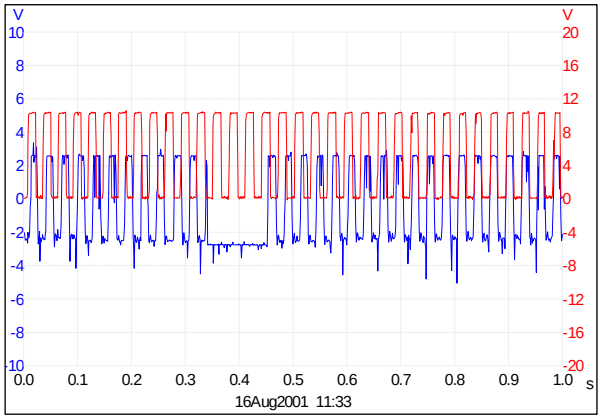

Figure 14 Feedback control signal (red) and inter-electrode gap voltage (blue) variation for EDM machining using the developed piezoelectric USM control system (gap current 5 A, gap voltage of 38 volts & duty cycle 4 μsec) [10]

It was observed, during this investigation, that the increment in the required level of current had no major influence on the stability of the developed piezoelectric servo feed drive system. Two factors showed an effect on the machining process, namely the sensitivity and the anti-arcing factor. The capability of changing the machining parameters during machining process was used in this investigation to select the optimum values, which provided a stable machining. It was noticed that mishandling the sensitivity and anti-arcing factors produced jerking effect led to unstable machining, which in turn increased the arcing and short-circuiting process and further causing poor surface profiles and increased the machining time. This was clear in the case of the electric servomotor feed drive system rather than the USM servo drive.

An electron microscopic investigation into the machined surface using EDM-system for both systems of control using current and developed system were carried out. **Figure 15** shows the leica Cambridge electron microscope used to investigate the microstructure of the machined surface using both systems of control. **Figure 17, Figure 18, Figure 19** and **Figure 20** show the scanning electron microscope image of the machined surface profiles using both servo drive control systems. It shows the investigations into the surface profiles machined using a different current level and duty cycle of 12 μsec. It can be seen clearly how the current level and duty cycle was used to control the machined surface finish as well as the difference between the surface profiles obtained using USM drive system and electric servomotor system. It can be seen that there is a smooth surface obtained using the developed system as clarified in **Figure 18** and **Figure 20**.

Figure 15 Leica Cambridge electron microscopes used to investigate the microstructure of the machined surface using both systems of control

The roughness of different machined surfaces using various electro-machining parameters was measured. In the case of machined holes it was difficult to achieve the measurements using normal equipment because of the need for a flat surface. Therefore the surface roughness in this case was measured using visual measurements using a comparator chart.

The chart was produced on a plate with a series of surface finishes. Comparison of the achieved surface with the chart

enabled an estimation of the surface's degree of roughness to be obtained. This shows that there is close agreement between the degrees of roughness using both servo systems of control. It also shows that the trend of the curve has a close agreement with the previous work [47]-[48] conducted on this area of machining. This was obtained with significant improvements in the surface profiles of the machined products.

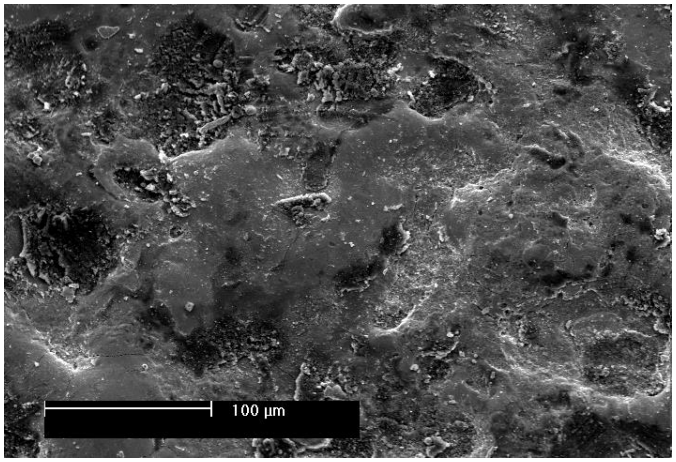

Figure 16 EDM surface finish obtained using DC servo control feed system using current level of 6 A, 'on' time of 50 µsec, duty cycle of 12 µsec [10]

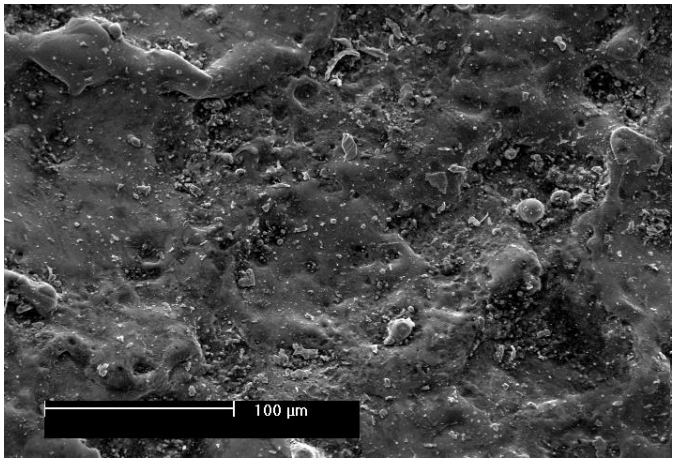

Figure 17 EDM surface finish obtained using USM servo control feed system using current level of 8 A, 'on' time of 50 µsec, duty cycle of 12 µsec [10]

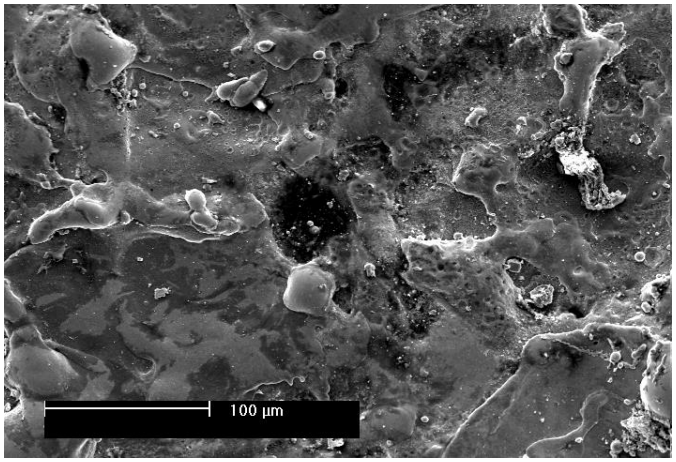

Figure 18 EDM surface finish obtained using DC servo control feed system using current level of 8 A, 'on' time of 50 µsec, duty cycle of 12 µsec [10]

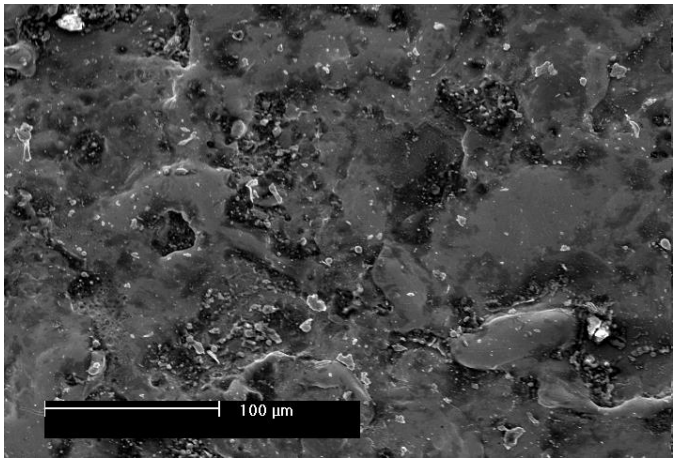

Figure 19 EDM surface finish obtained using USM servo control feed system using current level of 8 A, 'on' time of 50 µsec, duty cycle of 12 µsec [10]

Calculation of the material removal rate (M.R.R.) was carried out using material removal rate (9). The main parameters of the relation were obtained during machining process for various electro-machining parameters using both systems of control.

$$\text{M.R.R.}\left(\frac{\text{mm}^3}{\text{min}}\right) = \frac{\left[\text{workpiece weight loss (gram)}\right]\times 1000}{\left[\text{Density}\left(\frac{\text{gram}}{\text{cc}}\right)\right]\times\left[\text{Machining time (min)}\right]} \quad (9)$$

M.R.R. is the material removal rate. Density of the steel used in this calculation was 7.8 Mg/m^3 (gram/cc). The material removal rate was in mm^3/minute. The parameters used in calculation such as workpiece weight loss, density and machining time were in gram, Mg/m^3 (gram/cc) and minutes, respectively. **Figure 21** shows the relationship between the material removal rate and various machining parameters used for both systems.

This shows clearly the improvements in the material removal rate using USM servo control drive system when compared to the electric servomotors system. This is mainly due to the stability, fast dynamic response and high resolution of the USM servo drive system.

V. Conclusions

This paper presented the state of art of the latest development in electro-discharge machining system technology. It demonstrated how the ultrasonic technology renovates the system, and transfers its industrial applications into a new era. The existing and newly developed servo control feed drive

system has been installed and evaluated in EDM standard machine. Various machining parameters have been used in this investigation. These showed that USM servo control drive has improved the EDM system stability of machining and this was verified by examining the electrode movements, the variations in the inter-electrode gap voltage and current, and feedback control signals. The investigation into the surface finish machined using both systems for control showed that there was a clear improvement in the surface finish machined using USM system of control. A reduction in the arcing and short circuit process was also observed. The relationship between the electro-machining parameters of the system and surface finish parameters showed a close agreement to the known relationship of this application. These improvements showed the influence of piezoelectric USM technology in this field of electro-machinery technology. The variations of material removal rate for various electro-machining parameters for both systems of control using electromagnetic servomotor and USM was obtained and also has shown a close agreement with the known one with very minor difference.

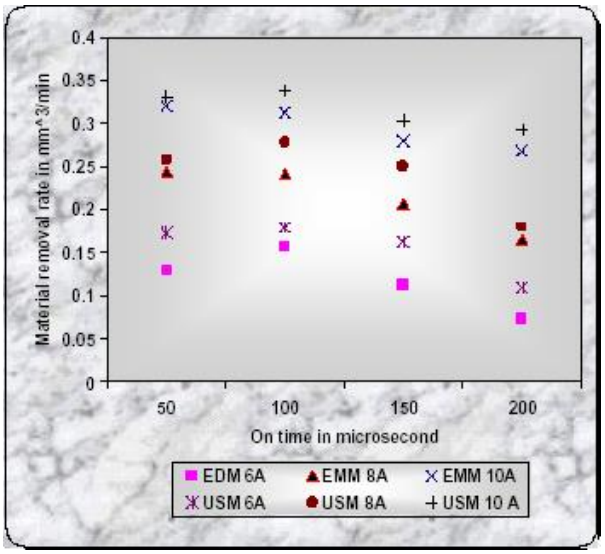

Figure 21 The variations of material removal rate for various electro-machining parameters for both systems of control using dc servomotor and piezoelectric USM [9]-[10], [18]-[20]

ACKNOWLEDGEMENTS

The author would like particularly to thank Professor J. Knight and Professor R. Bansevicius for their help, support, and constructive discussion throughout this research. My deepest thanks also goes to Professor S. Ahmed, and Mr. A. Smith for his guidance and endless support.

REFERENCES

[1] El-Menshawy, F., "Electro-discharge machining apparatus", United States Patent, Patent No. 4950860, August, 1990.

[2] Battacharyya, S. K., and El-Menshawy, F., "Monitoring and controlling the EDM Process", Trans. ASME, J. Eng. Ind., paper 79-WA/Proc-2, pp. 1-6, 1980.

[3] Battacharyya, S. K. and El-Menshawy, F., "Monitoring the EDM Process by radio signal", Int. J. Prod. Res., 16 (5), 353-63, 1978. CrossRef

[4] Aspinwall, D., Zhao, F., and El-Menshawy, F., "Electrical discharge texturing (EDT) of steel rolls", Surface topography 2, pp.123-141, 1989.

[5] Behrens, A., and Ginzel, J., "A comparison of different input values for gap-width controllers used in electro-discharge machining", 13th international symposium for Electromachining, ISEM, Spain, May 9th to 11th, 2001.

[6] Behrens, A., and Ginzel, J., "An open numerical control architecture for electro discharge machining", 13th international symposium for Electromachining, ISEM, Spain, May 9th to 11th, 2001.

[7] Behrens, A., Ginzel, J. and Bruhns, F., "Arc detection in electro-discharge machining", 13th international symposium for Electro-machining, ISEM, Spain, May 9th-11th, 2011.

[8] El-Menshawy, F. and Snaith, "Advances in electrical-discharge texturing (EDT) for cold mill work rolls", Iron and Steel Engineer, pp. 57-58, August, 1991.

[9] Shafik M., 'Computer Aided Analysis and Design of a New Servo Control Feed Drive for EDM using Piezoelectric USM', PhD Thesis, De Montfort University, Leicester, UK, 2003.

[10] Shafik M. and Abdalla H. S., 'A Micro Investigation into Electro Discharge Machining Industrial Applications Processing Parameters and Surface Profile Using a Piezoelectric Ultrasonic Feed Drive', ASME, J. Manuf. Sci. Eng. August 2011, Volume 133, Issue 4, 044503 (7 pages) DOI: 10.1115/1.4004687, USA, 2011. CrossRef

[11] Shafik M., Knight J. and Abdalla H. S., 'Development of a new generation of electrical discharge texturing system using an ultrasonic motor', 13th International Symposium for Electromachining, , Spain , ISEM, 9 -11 May 2001.

[12] M. Shafik & H. S. Abdalla, (2013), 'A New Servo Control Drive for Electro Discharge Texturing System Industrial Applications Using Ultrasonic Technology, International Journal of Engineering and Technology Innovation, vol. 3, no. 3, pp. 180-199, 2013.

[13] Simao J. and Aspinwall D., El-Menshawy F. and Ken Meadows K., 'Surface alloying using PM composite electrode materials when electrical discharge texturing hardened AISI D2', Journal of Materials Processing Technology, 127 (2), 211-216, 2002. CrossRef

[14] Behrens A., and Ginzel J., 'An open numerical control architecture for electro discharge machining', 13th international symposium for Electromachining, ISEM, Spain, May 9th to 11th, 2001.

[15] Behrens A., Ginzel J. and Bruhns F., 'Arc detection in electro-discharge machining', 13th international symposium for Electromachining, ISEM, Spain, May 9th to 11th, 2001.

[16] Lin F. J., Wai R. J. and Hong C. M., 'Recurrent neural network control for LCC-resonant ultrasonic motor drive', IEEE Trans. on ultrasonics ferroelectrics and frequency control, 47 (3): 737-749, May, 2000. CrossRef

[17] Izuno Y., Izumi T., Yasutsune H., Hiraki E. and Nakaoka M., 'Speed tracking servo control system incorporating travelling-wave-type ultrasonic motor and feasible evaluations', IEEE Transactions on Industry Applications, 34 (1): pp. 126-132, January-February, 1998.

[18] M. Shafik & E. M. Shehab & H. S. Abdalla, (2009) 'A Linear Piezoelectric Ultrasonic Motor Using a Single Flexural Vibrating Bar for Electro Discharge System Industrial Applications', The International Journal of Advanced Manufacturing Technology, Volume 45, Numbers 3-4, 287-299, DOI: 10.1007/s00170-009-1955-5, UK, 2009. CrossRef

[19] M. Shafik & H. S. Abdalla, Per Fransson, (2013), 'A Piezoelectric Servo-Drive for Electro Discharge System Industrial Applications Using Linear Piezoelectric Ultrasonic Motor', ASME J. Manuf. Sci. Eng. April 2013, Volume 144, Issue 2, 044503 (10 pages) DOI: 10.1115/1.4023707, USA, Mar 22, 2013. CrossRef

[20] M. Shafik & H. S. Abdalla, (2013),'A Smart Servo Feed Drive for Electro Discharge Machining Systems Industrial Applications Using Piezoelectric Technology', International Journal of Automation and Control Engineering, Volume 2, Issue 3, August, 2013.

[21] Izuno, Y., and Nakaoka, M., 'Ultrasonic motor actuated direct drive positioning servo control system using fuzzy reasoning controller', Electrical Eng. in Japan, Vol. 117, No. 6, pp. 74-84, 1996. CrossRef

[22] Ito K., Tsuji T., Kato A. and Ito M., 'EMG pattern classification for a prosthetic forearm with three degrees of freedom', Robot and Human Communication, Proceedings, IEEE International Workshop, DOI: 10.1109/ROMAN.1992.253907, 1992. CrossRef

[23] Lim K., Lee J. S. and Kang S. H., 'Characteristics of a iniaturized Ultrasonic Motor for Auto-focusing of a Mobile Phone', Journal of Electrical Engineering & Technology, Vol. 1, No. 1, pp. 106~109, 2006. CrossRef

[24] Furutani K. and Furuta A. March, 'Evaluation of driving performance of piezoelectric actuator with current pulse', 10th IEEE International Workshop on Advanced Motion Control, 26-28, 387-392, 2008.

[25] Zhang F., Chen, W., Lin J. and Wang Z., 'Bidirectional linear ultrasonic motor using longitudinal vibrating transducers', IEEE Transactions on Ultrasonics, Ferroelectrics and Frequency Control, 52(1), 134-138, 2005. CrossRef

[26] Chen Y., Lu K., Zhou T.Y., Liu T. and Lu C.Y., 'Study of a mini-ultrasonic motor with square metal bar and piezoelectric plate hybrid', Jpn. J. Appl. Phys., 45(5B), 4780-4781, 2006. CrossRef

[27] Li X., Chen W.S., Tang X. and Liu J.K., 'Novel high torque bearingless two-sided rotary ultrasonic motor', Journal of Zhejiang University - Science A, 8(5), 786-792, 2007.

[28] Frangi A., Corigliano A., Binci M. and Faure P., 'Finite element modelling of a rotating piezoelectric ultrasonic motor', Ultrasonics', 43(9), 747-755, 2005. CrossRef

[29] Aoyagi M., Tomikawa Y. and Takano T., 'Ultrasonic motors using longitudinal and bending multimode vibrators with mode coupling by external additional asymmetry or internal nonlinearty', Japanese J. of Applied Physics part 1, 31(9B), 3077-3080, 1992. CrossRef

[30] Aoyagi M. and Tomikawa Y., 'Ultrasonic motor based on coupled longitudinal-bending vibrators of a diagonally symmetry piezoceramic plate', Electronics and Communications in Japan, 79(6), 60-67, 1996.

[31] Chiharu K., Yoshiro T., Sadayuki T., and Takehiro T., 'Effect of the pressing force applied to a rotor on Disk type ultrasonic motor driven by self oscillation', Japanese journal of applied Physics, 37, 2966-2969, DOI: 10.1143/JJAP.37.2966. 1998. CrossRef

[32] Shafik M., 'Computer Simulation and Modelling of Standing Wave Piezoelectric Ultrasonic Motor Using Flexural Transducer', ASME 2012 International Mechanical Engineering Congress and Exposition, Houston, TX, USA, 2012.

[33] Shafik M., 'An Investigation into the Influence of Ultrasonic Servo Drive Technology in Electro Discharge Machining Industrial Applications', ASME 2012 International Mechanical Engineering Congress and Exposition, Houston, TX, USA, 2012.

[34] Ming Y. and Que P. W., 'Performance estimation of a rotary traveling wave ultrasonic motor based on two-dimension analytical model', Ultrasonics, 39(2) 115-120, 2001. CrossRef

[35] Lebrun L., Gonnard P. and Guinet M., 'A Low-cost piezoelectric motor using a (1,1) nonaxisymmetric Mode', Smart Mater. Struct. , 8(4), 469-475, DOI:10.1088/0964-1726/8/4/304, 1999. CrossRef

[36] Takano T., Tomikawa Y. and Takano C.K., 'Operating characteristics of a same-phase drive-type ultrasonic motor using a flexural disk vibrator', Japanes J. of Applied physics part 1- 1999, 38(5B), 3322-3326, 1999.

[37] He S., Chen W., Tao X., and Chen Z., 'Standing wave bi-directional linearly moving ultrasonic motor', IEEE Transactions on Ultrasonics, Ferroelectrics and Frequency Control, 45(5), 1133-1139, 1998. CrossRef

[38] Newton D., Garcia E., and Horner G. C., 'A Linear piezoelectric motor', Smart Materials and Structures, 6, 295-304, 1997.

[39] Zhang B. and Zhenqi Z., 'Developing a linear piezomotor with nanometer resolution and high stiffness', IEEE/ASME Transaction on Mechatron, 2(1), 22-29, 1997. CrossRef

[40] Tal J., Gyorki J., and ohn R., 'Servomotors take piezoceramic transducers for a ride', Machine Design; 12/09/99, Vol. 71 Issue 23, p92, 1999.

[41] Tobias H. and Wallaschek J., 'Survey of the present state of the art of piezoelectric linear motors', Ultrasonics, 38, 37-40, 2000. CrossRef

[42] Snitka V., 'Ultrasonic actuators for nanometer positioning', Ultrasonics, Vol. 38 issues (1-8), pages 20-25, March 2000.

[43] www.nanomotion.net

[44] Shafik M. & Knight J., 'Computer simulation and modelling of an ultrasonic motor using a single flexural vibrating bar', Proceeding of ESM'2002 International Conference, 3 – 5 June, Germany, 2002.

[45] Lin M. W., Abatan A. O. and Rogers C. A., 'Application of commercial finite codes for the analysis of induced strain-Actuated structures', Journal of Intelligent Material Systems and Structures, 5(6), 869-875., 1994. CrossRef

[46] Hwang W. S. and Park H. C., 'Finite element modelling piezoelectric sensors and actuators', *AIAA J*, 31(5), 930-937, 1993. CrossRef

[47] McGeough J. and Rasmussen H., 'A model for the surface texturing of steel rolls by electro discharge machining', Proceedings: Mathematical and Physical Sciences, 436, 155-164, 1992.

[48] El-Menshawy F., and Ahmed M. S., 'Monitoring and control of the electrical discharge texturing process for steel cold mill work roll', Proc. of 13th North American Research Conference, 470-475, 1985.